Journal of South American Earth Sciences 77 (2017) 42–50

Contents lists available at ScienceDirect

Journal of South American Earth Sciences

journal homepage: www.elsevier.com/locate/jsames

Mercury accumulation rates in Caço Lake, NE Brazil during the past 20.000 years

Luiz Drude de Lacerda [a, *], Bruno Turcq [b, c, e], Abdel Sifeddine [b, d, e], Renato Campello Cordeiro [d, e]

[a] Instituto de Ciências do Mar, Universidade Federal do Ceará, Fortaleza, 60165-081, CE, Brazil
[b] IRD-Sorbonne Universités, IPSL_ LOCEAN (UPMC-IRD-CNRS-MNHN), 32, Avenue Henri Varagnat, 93143 Bondy Cedex, France
[c] Universidad Peruana Cayetano Heredia, Av Honorio Delgado 430, San Martin de Porres, Lima, Peru
[d] Universidade Federal Fluminense (UFF), Departamento de Geoquímica, Morro do Valonguinho s/n, Niterói, RJ, Brazil
[e] LMI PALEOTRACES (IRD, UPMC, UFF, Uantof, UPCH), Departamento de Geoquímica, Morro do Valonguinho s/n, Niterói, RJ, Brazil

ARTICLE INFO

Article history:
Received 16 November 2016
Received in revised form
7 March 2017
Accepted 17 April 2017
Available online 20 April 2017

Keywords:
Paleoclimate
Tropical lake
Deposition
Mercury

ABSTRACT

Total Hg, TC, TN, goethite and siderite distributions in sediment cores from two locations across Caçó Lake (Brazil) identified paleoclimate factors that had affected the Hg deposition in this shallow tropical lake and its relationship with past climate and basin processes. Concentrations and fluxes of Hg were maximum in the Last Glacial Maximum (LGM), with averages of 397 ng g^{-1} and 24.3 μg m^{-2} yr^{-1}, respectively, decreasing during the Heinrich Stadial 1 (H1) and further during the Meltwater pulse 1A (MWP-1A). The higher values during LGM and H1 were strongly associated with dust deposition as observed in Greenland ice cores. After a period of lower values, there was a significant increase of concentrations and fluxes during the Younger Dryas (193 ng g^{-1} and 4.1 μg m^{-2} yr^{-1}), still associated in part with dust deposition but also being influenced by the high volcanic activity of this period. Concentrations and fluxes decreased again to the lowest values during the Holocene from about 9500 to 2000 cal yr BP (114 ng g^{-1} and 1.25 μg m^{-2} yr^{-1}). Analyses of ^{210}Pb dated shorter cores shows increasing Hg accumulation rates during the past century, larger than in other period in the past but could not evidence the influence of colonial gold mining as suggested by earlier studies.

1. Introduction

The accuracy of past (pre-industrial) Hg deposition rates are of key importance to modelling global Hg cycle. Recent models discerning anthropogenic and natural loads of Hg at a global scale needs these estimates to proper assess the effect of emissions control policies, since higher rates between natural, pre-industrial to industrial emissions would mean a longer time-delayed response to any reduction resulting from these policies (Engstrom et al., 2014).

Pre-industrial atmospheric Hg deposition estimates are mostly from historical archives measurements obtained from sediment cores from lakes and oceans, and vary greatly through time. Accumulation rates showed highly affected by past climate conditions, geography and basin processes and volcanism. During the Holocene, accumulation rates of Hg in the Amazon region varied by a factor of up to 3 after the LGM (Late Glacial Maximum) between 15,000 and 2000 cal yr BP and were higher relative to Pleistocene values, between 41,000 and 26,000 cal yr BP (Santos et al., 2001; Barbosa et al., 2004). These studies however, presented gaps in the sedimentation history extending thousands of years, in particular during the period when deglaciation processes occurred. Roos-Barraclough et al. (2002) also showed Hg deposition rates during the Holocene and Late Glacial in southern Europe with significantly higher Hg deposition during the Younger Dryas relative to deposition rates observed in layers deposited before and after this period, but the study was restricted to the past 15,000 years only. These studies showed good association between Hg deposition rates and climate. Therefore, Hg concentrations and fluxes in sediment cores are useful proxies to the investigation of climate changes in particular in regions with scarce data on paleoclimatological history, such as in northeastern Brazil.

Apart from climate change, several authors have identified

* Corresponding author. Laboratório de Biogeoquímica Costeira, Instituto de Ciências do Mar, Universidade Federal do Ceará, Fortaleza, 60165-081, CE, Brazil.
E-mail address: ldrude@fortalnet.com.br (L.D. de Lacerda).

http://dx.doi.org/10.1016/j.jsames.2017.04.008
0895-9811/

sharp increases in Hg concentrations and fluxes associated with volcanic eruptions. Since explosive emissions reach tropospheric levels and the residence time of Hg in the atmosphere is relatively long (1–2 years), volcanic influences can affect Hg deposition rates worldwide (Pyle and Mather, 2003). These peaks were observed in many historical archives from peat bogs, lake sediments and glacial ice (Roos-Barraclough et al., 2002), recording relatively modern eruptions, as well as Holocene volcanic activities, and may difficult the interpretation of the impact of climate change on Hg deposition. Moreover, the late Holocene witnessed increasing deposition rates firstly due to increasing frequency of forest fires (Cordeiro et al., 2011), then to the onset of precious metals mining using Hg amalgamation (Lacerda and Salomons, 1998) and latter with the industrial revolution (UNEP, 2013; Engstrom et al., 2014).

Unfortunately, detailed information for the so-called Termination 1, or the Late Glacial, a period covering the major events of the last deglaciation, is still scarce to fully understand the process underlying the variability of Hg deposition rates. This study presents the distribution of Hg concentrations and fluxes, as well as proxies of climate changes and of basin processes in a shallow, remote tropical lake, Lake Caçó, in Northeastern Brazil, and proposes mechanisms responsible for their variability.

2. Material & methods

Lake Caçó (Fig. 1) is located in Maranhão state, northeastern Brazil, on the eastern border of the Amazon basin, about 80 km from the Atlantic coast at 2°58′ S, 43°25′ W, 80 m altitude. The lake occupies a former river valley in a Pleistocene dune field presently covered by *cerrado* (shrub savannah) vegetation. The weather in the region is tropical, semi-humid, with an annual dry season extending for 4–5 months. Average annual temperature is 26 °C, with daily averages between 36 °C in the austral summer and 16 °C in the winter. Annual rainfall ranges from 1500 to 1750 mm and is essentially controlled by seasonal shifts in the position of the Inter-Tropical Convergence Zone.

A bathymetric map shows that the lake occupies a rectilinear valley between old longitudinal aeolian dunes (Fig. 1). A newer generation of small barchans developed on the longitudinal ridges. The vegetation today fixes both aeolian dune generations. Northeast trade winds are responsible for constant mixing of the water column and a detailed physicochemical investigation identifies the lake as polymictic with unstable water column stratification. It is presently oligotrophic to meso-oligotrophic, with only very low phytoplankton growth. Today lake margin wetlands constitute a biological- and nutrients-rich zone that excludes most or even all the mineral discharge from the sandy margins of the lake, but exports part of its own production to the lake center. A 2 m thick floating meadow at the lake entrance filters most of the mineral and organic influx from the small tributary. Thus, inorganic sedimentation consists mostly of aeolian particles and authigenic minerals (Sifeddine et al., 2011).

The bulk organic matter in Lake Caçó sediment cores and its palinological record observed by Sifeddine et al. (2003) reflect variations in delivery and preservation of the organic matter that suggest the local climate fluctuated over the past 20,000 years, with drier intermixed with wetter periods than today (Ledru et al., 2001).

One long (300 cm deep) and two short (top 40 cm) cores were collected in the lake. Fourteen AMS radiocarbon dating (Table 1) were determined on the total organic matter from 1 or 2 cm-thick layers, cut from the 304 cm-long core (MA97-1) sampled in the deepest sector of the lake, at Beta Analytics and NSF Arizona AMS Facility. The radiocarbon ages were calibrated by using the program CALIB 5.02 (Stuiver and Reimer, 1993).

Probability peak of the calibration curve in each 2-sigma (2σ) interval was assumed to calculate the age model based on polynomial interpolations (Fig. 2). Two shorter cores (~35 cm) were collected at shallower depths from the lake margins to better interpret recent variability of Hg deposition. There was no dating in these cores but we used the sedimentation rate obtained by analyses of excess ^{210}Pb, in a short core in the same region to approximate Hg fluxes. Obtained sedimentation rates were multiplied by the sediment bulk density of each sediment layer and the respective Hg concentrations, in order to estimate Hg deposition rate.

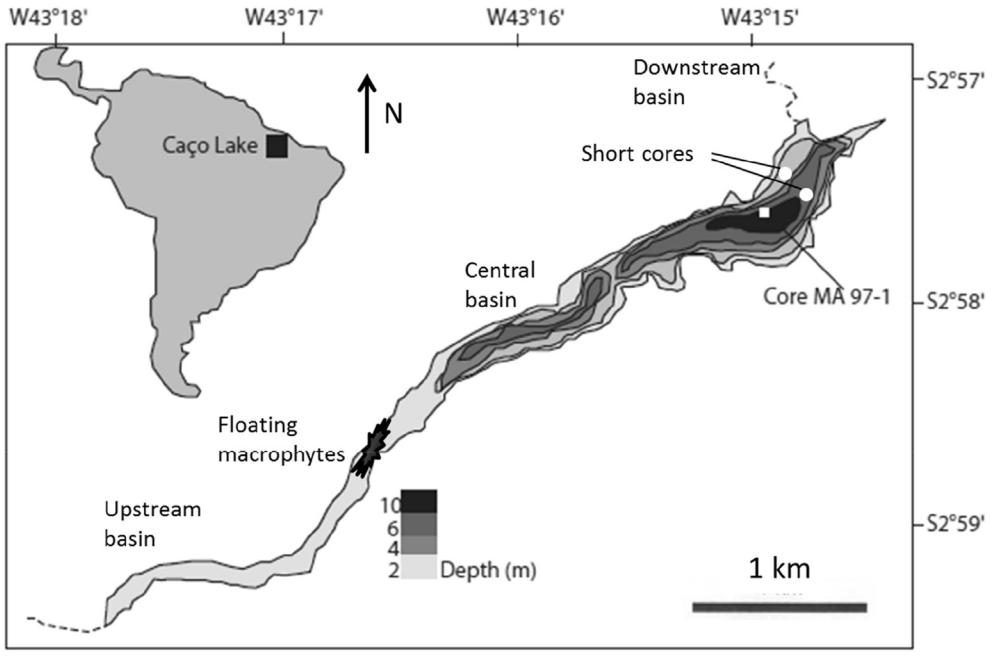

Fig. 1. Map showing the location of cores retrieved from Lake Caçó in Northeastern Brazil.

Table 1
Carbon 14 and calibrated ages from 14 depths along core MA97-1 from Lake Caçó, Northeastern Brazil.

Ages ^{14}C BP	Depth (cm)	Calibrated Ages
3060 ± 50	21	3260
3780 ± 50	32	4110
5000 ± 60	43	5740
5584 ± 78	49	6350
6010 ± 50	69	6860
7600 ± 50	98	8370
9040 ± 95	138	9990
10880 ± 50	173	10960
11605 ± 120	179	12800
12390 ± 90	201	13530
12640 ± 135	217	14860
13880 ± 155	242	15320
15400 ± 180	260	16650
15870 ± 60	276	18320

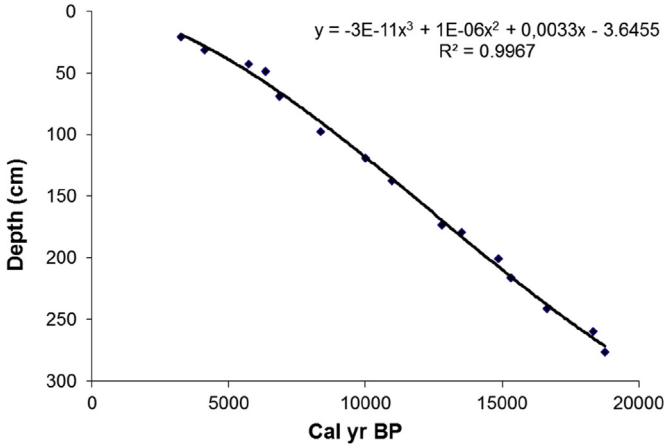

Fig. 2. Depth-age calibration curve showing equation used to estimate sedimentation rates in the MA97-1 core from Caço Lake.

Goethite, siderite and quartz were quantified by Fourier Transformed Infrared Spectrometry (Perkin Elmer 16 PC FTIR), following the method described by Bertaux et al. (1998).

Total carbon (TC) and nitrogen (TN) concentrations compositions were measured on dried whole sediment samples by combustion with a LECO analyzer. Because sediments of Lake Caçó contain no $CaCO_3$ (Sifeddine et al., 2003; Jacob et al., 2004), the whole-sediment results generally correspond to bulk organic matter elemental compositions with exception of three siderite peaks that have been evidenced by Fourier Transformation Infrared Spectroscopy (Fig. 3).

For determination of total Hg concentrations, homogenized 0.5–1.0 g samples of sediments, dried at 40 °C to constant weight, were digested with an acid mixture (50% *acqua regia* solution), and heated at 70 °C for one hour, in a thermal-kinetic reactor "cold finger". Glass and plastic ware were decontaminated by immersion for 2 days in 10% (v/v) Extran solution (MERCK), followed by immersion for 3 days in diluted HNO_3 (10% v/v) and final rinsing with Milli-Q water. All chemical reagents used were of at least analytical grade. Cold Vapor Atomic Absorption Spectrophotometry quantified Hg concentrations, after Hg^{2+} reduction with $SnCl_2$. Duplicates in all samples showed reproducibility within 9.5%. A certified reference material (NRC PACS-2, Canada) simultaneously analyzed to evaluate Hg determination accuracy, showed good precision, as indicated by the relative standard deviation of three replicates, and Hg recovery of 98.8 ± 6.2%. The Hg detection limit estimated as 3 times the standard deviation of reagent blanks, was 1.26 ng g^{-1}. In all cases, blank signals were lower than 0.5% of sample analysis. Concentration values were not corrected for the recoveries found in the certified material.

3. Results

Fig. 3 shows the vertical distribution of total carbon (TC), C/N ratios, goethite and Hg concentrations. At least 5 major periods can be identified roughly based on siderite concentrations, which implies changes in redox state of the sediment. Highest, but highly variable Hg concentrations with an average of 397 ng g^{-1} (148–730 ng g^{-1}) were observed from the bottom of the core to about 243 cm (Unit V). Lowest total carbon and goethite concentrations occurred in this interval. Above this depth, Hg concentrations decreased and remained relatively constant with an average of 282 ng g^{-1} (119–403 ng g^{-1}) to about 210 cm (Unit IV). Total carbon and goethite steadily increased up to 170 cm (Unit III), although Hg concentrations from 210 to this depth varied from 102 to 218 ng g^{-1} with an average of 157 ng g^{-1}. From 169 to 95 cm (Unit II) concentrations were higher and relatively constant varying from 130 to 310 ng g^{-1} (average of 193 ng g^{-1}). Total carbon and goethite concentrations decreased along this interval. From 95 cm to the top (Unit I) of the core Hg concentrations were lowest (average 114 ng g^{-1}), but showing a continuous increase to the top from minimum values of about 50 ng g^{-1} in the deepest part of this section and highest of about 200 ng g^{-1} at the surface. Total carbon and goethite concentrations remained relatively constant along the top 100 cm of the core, but decreased significantly at the top 20 cm of the core.

Peaks of TC/TN ratios occurred in three different depths along the core at 160 cm, 200 cm and 240 cm; these peaks are associated with elevated concentrations of inorganic carbon from siderite ($FeCO_3$) rather than significant changes in organic matter production or load to the lake. Both siderite and goethite are formed by authigenic precipitation in the lake (Sifeddine et al., 2003). The occurrence of discrete peaks of siderite may indicate more anoxic conditions needed for iron reduction and less acidic conditions of sediment pore water than during goethite formation (e.g. Fritz and Toth, 1997). The age of siderite is the same, in the limit of 1 sigma error than the age of surrounding sediment (between 17,880 and 14,650 cal yr BP for the siderite, 17,020 and 16,710 cal yr BP for the sediment) showing that the siderite probably precipitated in the first cm of the sediment.

Sedimentation rates throughout the core were relatively constant and varied by a factor of 2; from 0.0062 to 0.0072 cm yr^{-1} in the top 50 cm of the core, increasing steadily to 0.0147 cm yr^{-1} in the bottom layers. Therefore, since Hg concentrations varied by a factor of 7, changes in concentrations reflects deposited material with different Hg concentrations, rather than different accumulation due to different sedimentation rates, as have been reported for lakes in eastern Amazonian lakes were very low sedimentation rates result in high Hg concentrations irrespectively of the type of sediments being deposited (Lacerda et al., 1999; Cordeiro et al., 2011).

Fig. 4 shows the vertical distribution of kaolinite and quartz, compared to Hg concentrations along core MA97-1. From the bottom of the core to about 250 cm (Unit V), sediments deposited in Lake Caçó, kaolinite and quartz makeup nearly 80% in weight of the sediment. This sediment layer also presented the highest Hg concentrations, suggesting strong transport of Hg-rich material to the lake probably adsorbed on clays. This is in agreement with the lowest total carbon values in the same depths (see Fig. 3) ruling out any increase of Hg deposition due to increasing primary production transferring more Hg to sediments as shown for present lake sediments (Carrie et al., 2010).

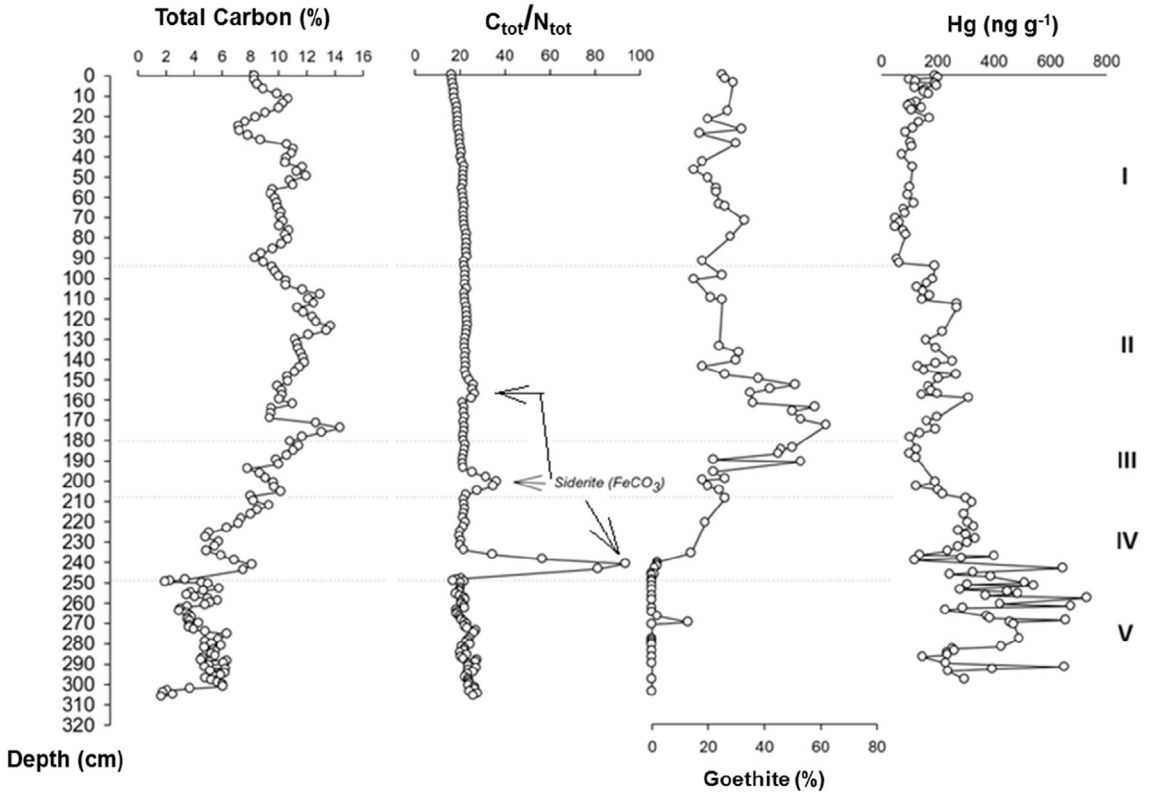

Fig. 3. Distribution of Hg, total carbon and goethite concentrations and C/N ratios in core MA97-1 from Lake Caçó, Northeastern Brazil.

Above 250 cm, Hg concentrations, kaolinite and quartz contents decreased, up to 200 cm. From this depth to the top of the core, covariation between Hg and quartz and kaolinite is weaker, suggesting a dominance of atmospheric deposition over basin and further transport. At the top 50 cm, quartz and kaolinite contents decreased whereas Hg concentrations increased.

4. Discussion

Mercury concentrations in the LGM section of the lake Caçó core suggest a transport of Hg-enriched materials to the lake. Since no Hg-bearing geology exists in the region and sedimentation rates are relatively constant, this enrichment results of the deposition of Hg-rich material from the atmosphere, related to global conditions followed by erosion and transport to the lake. Fig. 5 shows Hg concentrations and calibrated ages compared to global climate proxies reproduced form Greenland ice records of dust and volcanic sulphate for the Termination 1 period (Billups, 2015). Recently, Lambert et al. (2008) reported the same pattern of dust deposition in Antarctica, suggesting a global phenomenon of larger atmospheric dust inputs during the LGM. The higher Hg concentrations during the LGM, from the bottom of the core to about 18,000 cal yr BP, in Lake Caçó are in accordance with heavy dust deposition recorded form Greenland ice (Zielinski and Mershon, 1997) and Antarctica (Lambert et al., 2008; no shown in Fig. 5). Colder and dryer climate during the glaciation resulted in a larger load of atmospheric particles, which scavengers Hg from the atmosphere in a similar manner as does soot from forest burning which increases atmospheric Hg deposition over the Amazon, as observed from Late Holocene records (Cordeiro et al., 2011), as well as today (Hacon et al., 1995; Cordeiro et al., 2002). During the Henrich Stadial 1 (H1) both dust in Greenland and Hg concentrations in the Caço Lake sediments decreased to minimum values reached at the MWP-1A and increased again during the Younger Dryas. Additionally, recent finding from peat bogs in Central Brazil (Pérez-Rodríguez et al., 2015) and from lake sediments from southern Chile (Hermanns and Biester, 2013), suggested that Hg deposited in these watersheds may be preferentially leached from soil resulting in relatively higher concentrations in bottom sediments. From Dome C core in Antarctica, Vandal et al. (1993), observed a triple of Hg concentrations between 27,000 and 17,000 ^{14}C yr BP relative to younger and older ice layers. The authors suggested higher oceanic productivity in this period as the major driver of increasing Hg emission to the atmosphere and further deposition.

Both LGM and H1 Hg concentrations were characterised by sharp, higher concentrations peaks compared to any other more recent period. Simultaneously total carbon concentrations during these periods were lowest (Fig. 3), suggesting low biological productivity. Therefore, highest Hg concentrations are rather the result of depositing Hg-rich matrices rather than higher bioaccumulation, leading to high Hg removal from the water column. Large land-water transport of materials to the lake from the surrounding basin, also evidenced by the increasing quartz and kaolinite contents observed in these sediment layers (Fig. 4) suggest alloctonous sources of Hg. However, this is also consistent with higher oceanic productivity and therefore Hg emissions to the atmosphere and eventual deposition. Although not ruling out increased oceanic primary production, our results suggest this driver as of minor significance, relative to its impact on Antarctica Hg deposition evidenced by Vandal et al. (1993).

Although during the LGM and H1, Hg concentrations followed the dust curve, during the Younger Dryas and MWP-1B, only a general synchronous trend is observed between the two curves. Many abrupt increases in Hg concentrations may be rather due to volcanic emissions, which although not enough to substitute the climate signal, blur it with more frequent volcanic activities during

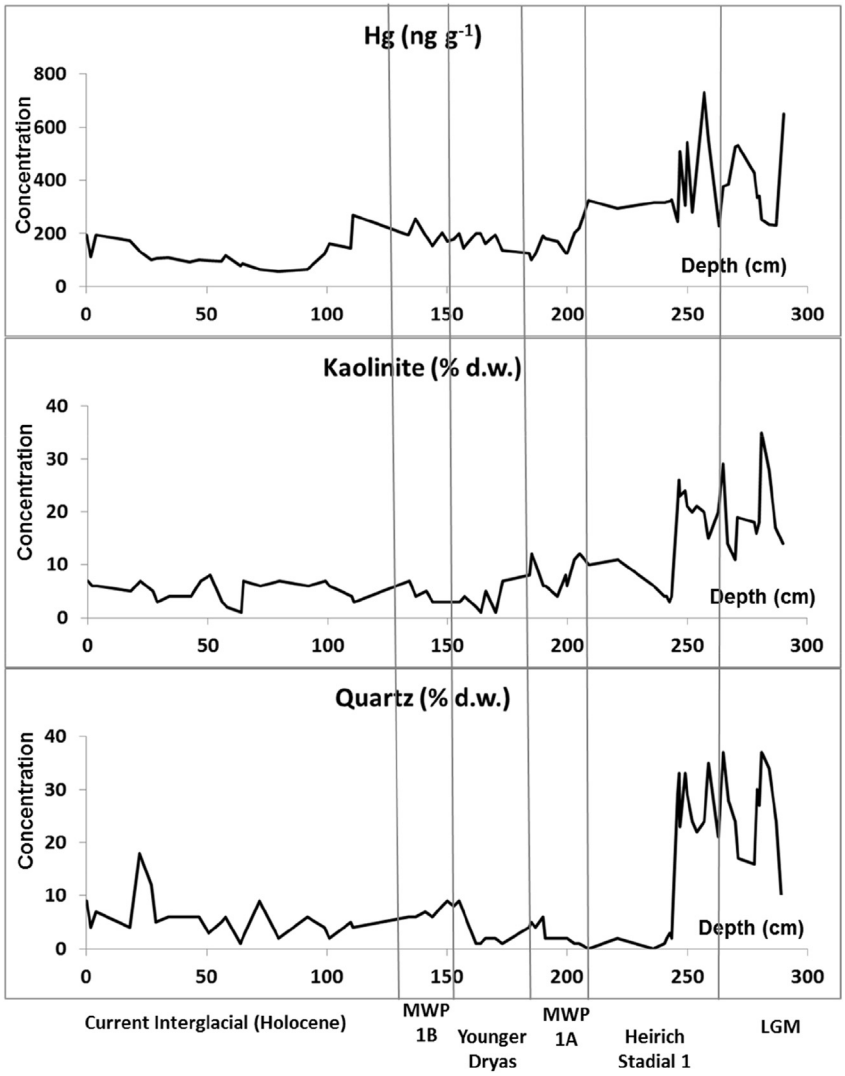

Fig. 4. Kaolinite, quartz and Hg concentrations in MA971 sediment core from Lake Caçó, Northeastern Brazil.

these periods, as seen from the higher volcanic sulphate concentrations. The period between 17,000 and 6000 cal yr BP is considered as of maximum volcanic activity during the late Quaternary (Zielinski et al., 1996; Mayewski et al., 1997). Bay et al. (2006), based on ash and SO_4 deposition from Antarctica and Greenland ice cores, also recorded the chronology of volcanism during the last 45,000 years BP suggesting the same period as of highest volcanic activity. Explosive volcanic emissions have been associated with peaks in Hg deposition recorded in modern sediments, such as the observed 18-fold increase relative to background deposition observed in the glacial ice core of the Upper Fremont of the Krakatau and Tambora eruptions (Schuster et al., 2002). In Holocene deposits, Roos-Barraclough et al. (2002) observed Hg peaks of over 10-fold the local background in Jura Mountains peat bogs, associated with intensive volcanic activity in Europe around 6000 BP. Pre-historic deposits as earlier as the Permian-Triassic boundary associated with Siberian traps volcanism (Sanei et al., 2012; Grasby et al., 2013) and the Cretaceous-Paleogen transitions associated with Deccan Phase 2 volcanism (Sial et al., 2013, 2014), also showed extremely high Hg peaks.

Lower Hg concentrations characterize the MWP-1-A but there is a small increase during the Younger Dryas. Similar peaks in Hg concentrations during the Younger Dryas, were reported by Roos-Barraclough et al. (2002), and were associated with an increase in dust deposition, lower temperature and probable increased oceanic emissions. During the MWP-1B and the late Holocene, Hg concentrations were the lowest, following in the general Calcium curve (Fig. 5). However, volcanic emissions may influence some of the Hg peaks during this period at least to about 5000 BP. From about 8500 BP to present Hg concentrations increased steadily to reach the highest values in this period at the core surface, and do not follow any global proxy of climate or volcanic activity.

Fig. 6 shows the Hg fluxes along the entire core based on dating shown in Table 1. Fluxes varied by a factor of 6 roughly following the distribution of Hg concentrations. Large Hg fluxes occurred through the LGM and H1 from the bottom of the core to about 14,500 BP, with average fluxes of 24.3 $\mu g\ m^{-2}\ yr^{-1}$ (4.9–61.2 $\mu g\ m^{-2}\ yr^{-1}$). Similar average Hg deposition fluxes to lake sediment in southern Chile between 17,300 BP to 10,800 cal yr BP reached 29.6 $\mu g\ m^{-2}\ yr^{-1}$ (Hermanns and Biester, 2013). Smaller fluxes from 2 to 3 times those of the LGM occurred at the end of the H1 period, but still larger than in any other later period. The magnitude of this fluxes' increases from the end of H1 to full LGM was also recorded in Antarctica ice core by Vandal et al. (1993) and Jitaru et al. (2009) (Fig. 7), suggesting, at least, a hemispheric phenomenon. In a peat mire in central Brazil, Pérez-Rodríguez et al. (2015) also found

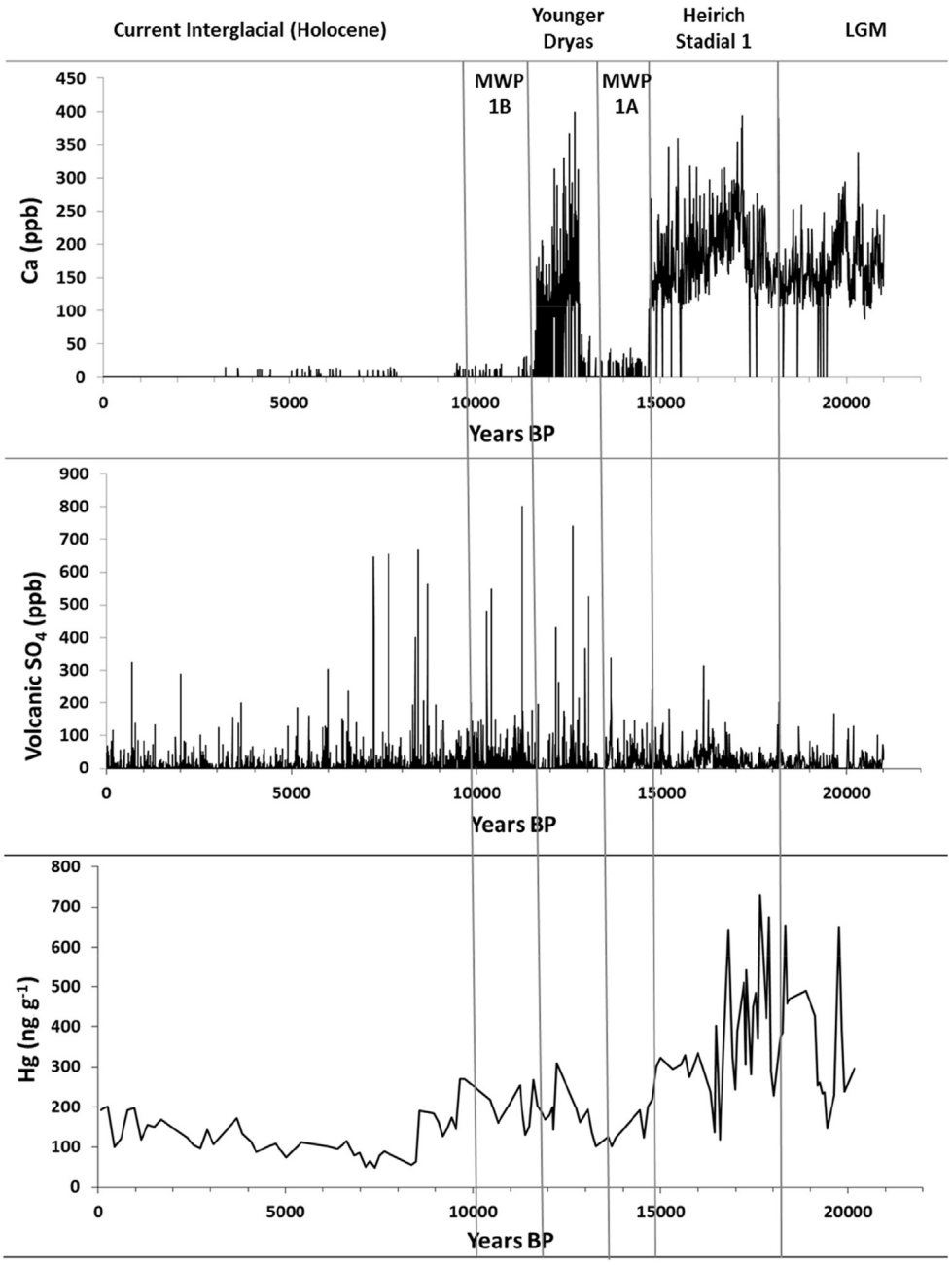

Fig. 5. Greenland ice core record of atmospheric deposition of dust and volcanic SO_4 (Taylor et al., 1996; Zielinski and Mershon, 1997; Zielinski et al., 1996; Mayewski et al., 1997) and Hg concentrations during Termination 1 (Time intervals according to Billups (2015)); compared to the Hg concentrations in MA971 sediment core from Lake Caçó, Northeastern Brazil.

maximum Hg fluxes during this period and attributed them to increase transport of material from the bog' basin. Unfortunately, absolute deposition rates reported by both studies derived from ice and peat cores, respectively, and cannot be comparable to our fluxes estimated from lake sediments.

Fluxes observed between 13,000 cal yr BP and 9500 cal yr BP varied from 2.23 to 7.75 μg m^{-2} yr^{-1}, with an average of 4.1 μg m^{-2} yr^{-1}. Peak fluxes (6.68–7.75 μg m^{-2} yr^{-1}) occurred during the Younger Dryas, around 11,600 BP, similar to a positive excursion reported by Pérez-Rodríguez et al. (2015) in central Brazil. Peak Hg fluxes during the Younger Dryas have also been recorded in the northern hemisphere (Roos-Barraclough et al., 2002). Again, these studies were based on peat bog cores impeding direct comparisons of absolute accumulation rates.

Smallest fluxes occurred since 8500 years BP and presented an average of 1.25 μg m^{-2} yr^{-1} (0.71–2.29 μg m^{-2} yr^{-1}). During this period, the highest Hg fluxes occurred at the top of the core. This range of fluxes agrees with pre-anthropogenic fluxes recorded for remote lakes in North America, which vary according to regional differences in atmospheric deposition from 1.5 μg m^{-2} yr^{-1}, measured in Arctic lakes; 3.0 μg m^{-2} yr^{-1}, in higher latitudes, to 7.2 μg m^{-2} yr^{-1} in Central North America (Engstrom et al., 2014). In South America, peat bog records from southern Chile recorded higher pre-anthropogenic fluxes of 2.5–3.9 μg m^{-2} yr^{-1} (Biester et al., 2002); lake sediment records from the same region were even higher (29.0 μg m^{-2} yr^{-1}) (Hermanns and Biester, 2013).

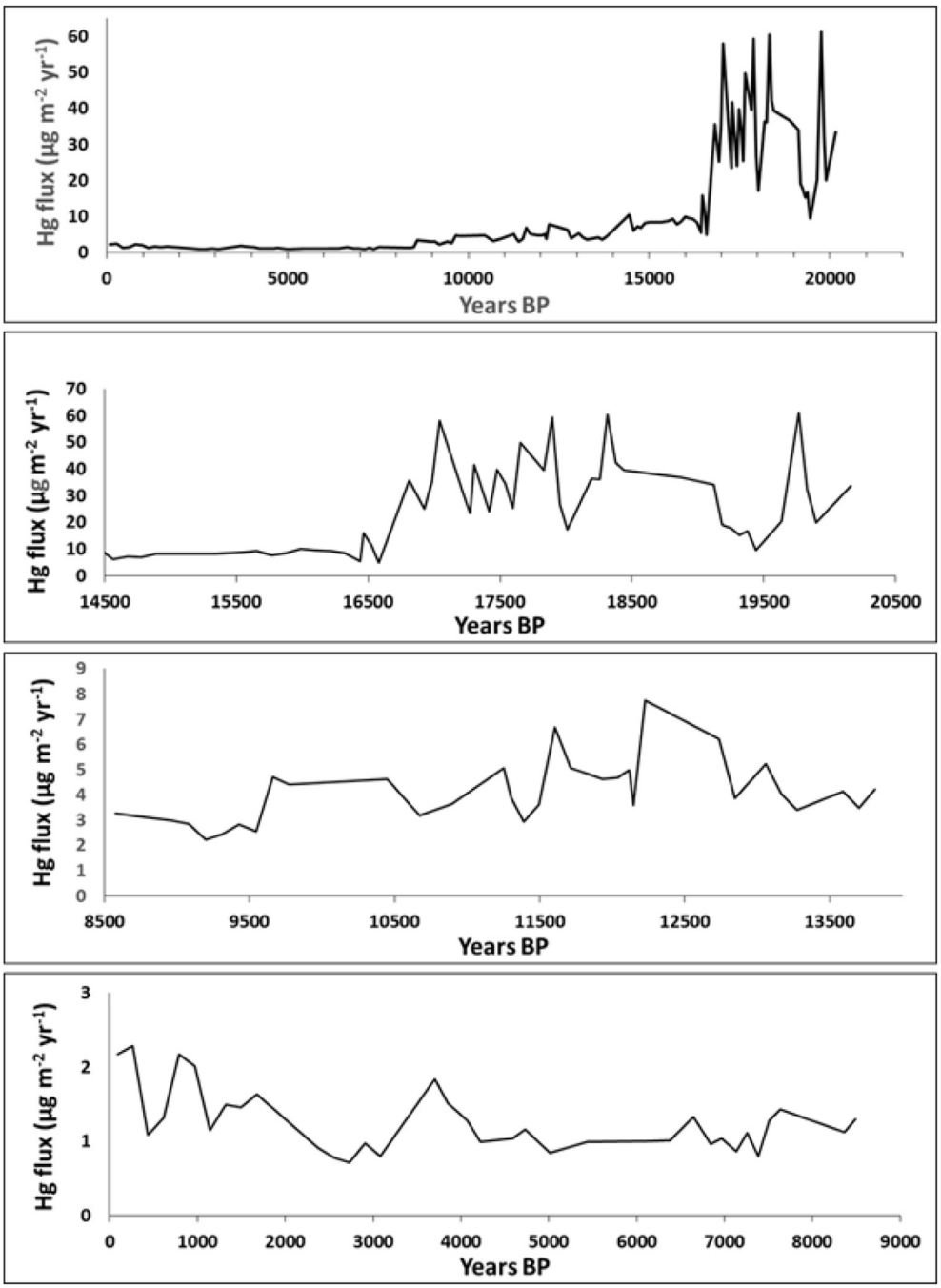

Fig. 6. Mercury fluxes through MA97-1 core from Lake Caçó, Northeastern Brazil during the past 20,000 years.

However, mire deposits from Central Brazil (Pérez-Rodríguez et al., 2015) gave much lower values (0.4–5.6 µg m^{-2} yr^{-1}), similar to those found in the Lake Caçó.

From contrasting latitudes in South America, Lacerda et al. (1999), in the Amazon, and Biester et al. (2002), in Southern Chile, reported an anthropogenic signal on the Hg accumulation rates in lake sediments from the Late Holocene. Pre-colonial use of Hg by South American civilizations, colonial mining followed by industrialization and, more recently, small scale gold mining, have been listed as probable source for this signal (Sun et al., 2006). Not all sources have been reported for all locations simultaneously which may suggest different geographical scales of influence of the different sources (see Engstrom et al., 2014; for a detailed discussion).

Unfortunately, sediment deposition in Lake Caçó seems to be very slow since 2000 cal yr BP (Sifeddine et al., 2011). In Core MA97-1 coherent dating was not obtained for the first 20 cm layer, which makes interpretation of historical Hg fluxes distribution in this core very difficult. In the shorter cores collected close to MA97-1; the presence of unsupported ^{210}Pb in the first 20 cm suggest that this narrow deposition layer may cover about 100 years. Sedimentation rates within this 20 cm layer were larger than in the MA97-1, with average rate of 0.134 cm yr^{-1} if assumed constant through the period. Fig. 8 shows concentrations and accumulation rates of Hg from the two short cores collected in Lake Caçó. Concentrations were relatively constant, of about 40–60 ng g^{-1}, from

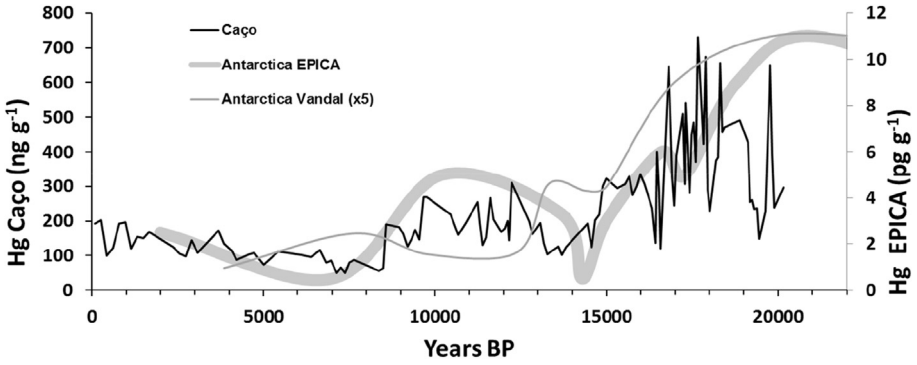

Fig. 7. Comparison of reported Hg concentrations in Caço Lake and Antarctica EPICA Dome C ice core from Jitaru et al. (2009) and Vandal et al. (1993) also from Dome C ice core, in Central Antarctica.

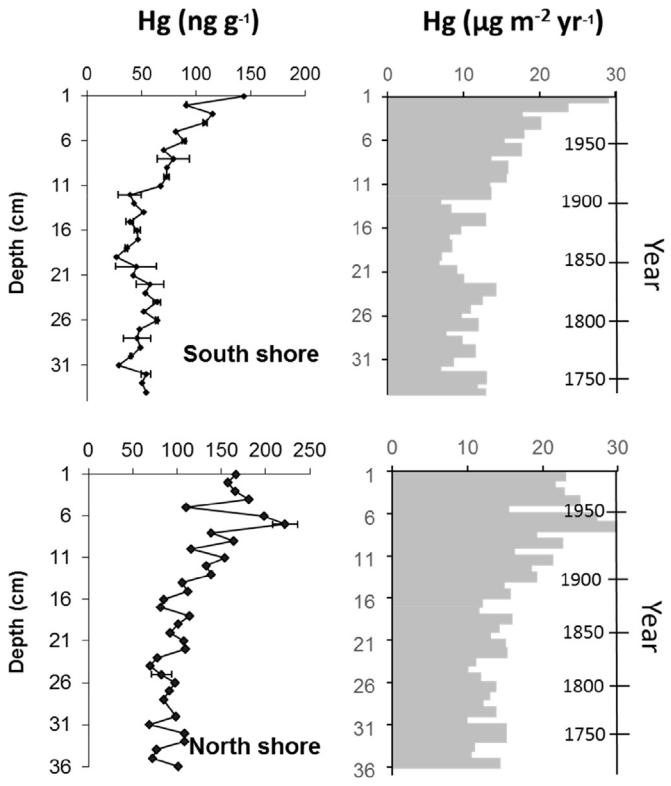

Fig. 8. Concentrations and accumulation rates of Hg in the past 150 years in Lake Caçó, northeastern Brazil. Dating prior to 1840 are only a gross estimate and are not included in the graph.

bottom to about 15 cm in both cores, resulting in Hg accumulation rates of about 15 μg m^{-2} yr^{-1}, corresponding to the earlier 20th century. Although the projected dates have to be taken with care, since we have considered a constant sedimentation rates for the past 100 years. From that depth Hg concentrations increased 3-fold at the surface of the cores, whereas accumulation rates also increased to 22.6–29.5 μg m^{-2} yr^{-1}. Similarly, accumulation rates of Hg in a peat bog in south Chile, reveal a 2.5-fold increase in the past 100 years (Biester et al., 2002), which is comparable to the accepted 3-fold increase in atmospheric Hg concentrations due to anthropogenic activities, notwithstanding the remoteness of the site and support the significance of long range atmospheric transport of Hg.

Lacerda et al. (1999) reported an increase of Hg accumulation rates of 0.7–2.6 μg m^{-2} yr^{-1} before 1600 AD to a maximum of 10 μg m^{-2} yr^{-1} in 1990 AD in lakes from the amazon region. This increase was associated with Spanish Silver and Gold Mining in the Americas, from 1540 to 1820 AD and to a further input in more recent times from small scale gold prospecting in the Amazon (Lacerda and Bastos, 2012). In Southeast Brazil, the highest Hg accumulation rates occurred in industrial times in the 1960s and 1970s with maximum (uncorrected) accumulation rates of 20–30 μg m^{-2} yr^{-1} in the 1990s (Lacerda and Ribeiro, 2004). These results suggest pre-industrial anthropogenic Hg deposition due to gold and silver mining using Hg amalgamations (Strode et al., 2009). As such, Hg deposition should have increased staring about 1540 AD when the "Patio" amalgamation technology was introduced in 1554 by Bartolomeu de Medina, first in Mexico and expanding rapidly to Peru and Bolivia (Lacerda and Salomons, 1998) and increased further in the late 1800s with the North American gold rush (Nriagu, 1994). Engstrom et al. (2014) have recently discussed the validity or at least the geographical limitation of this model. They argued that most of Hg released by the colonial gold and silver mining deposited on a local scale, due to the amalgamation technique then in use, rather than on a regional or global scale, such as in today gold rush. Our results from Caço Lake, support this view since no peak in Hg deposition was found in this remote lake, outside the local and even regional area of influence of the colonial gold mining. Rather the increasing deposition rates are consistent with the global increase in Hg atmospheric emission observed after the industrial revolution.

5. Conclusions

Mercury concentrations and deposition in this Equatorial lake over the past 22,000 years responds to processes resulting from global changes in atmospheric dust and climate during the last deglaciation and global volcanism. The high atmospheric dust content during the glacial period has favored mercury deposition in Caço Lake watershed by atmospheric scavenging. This mercury is transferred to the lake sediment by run-off during the LGM. During Heinrich event 1 the mercury flux was still high maintained by the high atmospheric dust deposition. A second period of high mercury concentration and flux is observed between 13,000 and 9500 cal yr BP. Although this period includes the Younger Dryas episode (13-12,000 cal yr BP) when global atmosphere dust concentration was high again, this longer interval better corresponds to higher global volcanic activity increasing atmospheric Hg. As in most other remote areas Caço Lake also preserve the anthropogenic signal of industrialization, but not of the colonial mining activity, as verified in lakes closer to the major mining districts of the 17ths and 18ths, suggesting that the inclusion of the large Hg emissions from

colonial mining to global models must be reinterpreted.

Acknowledgements

Funding was provided by CNPq-INCT-TMC*Ocean* Project (Proc. No. 573.601/2008-9) and PECI-CNPq 402.428/2012-9. We deeply think the cooperative project PRIMO (CNPq-IRD) and International Joint Laboratory "PALEOTRACES".

References

Barbosa, J.A., Cordeiro, R.C., Silva, E.V., Turcq, B., Gomes, P.R.S., Santos, G.M., Sifeddine, A., Albuquerque, A.L.S., Lacerda, L.D., Hausladen, P.A., Tims, S.G., Levchenco, V.A., Fifield, L.K., 2004. ^{14}C-MAS as a tool for the investigation of mercury deposition at a remote Amazon location. Nucl. Instrum. Methods Phys. Res. B 223/224, 528–534.

Bay, R.C., Bramall, N.E., Price, P.B., Clow, G.D., Hawley, R.L., Udisti, R., Castellano, E., 2006. Globally synchronous ice core volcanic tracers and abrupt cooling during the last glacial period. J. Geophys. Res. 111, D11108. http://dx.doi.org/10.1029/2005JD006306.

Bertaux, J., Frohlich, F., Ildefonse, P., 1998. A new application of FTIR spectroscopy for the quantification of amorphous and crystallized mineral phases. Example of organic rich sediments. J. Sediment. Res. 68, 440–447.

Biester, H., Kilian, R., Franzen, C., Woda, C., Mangini, A., Scho, H.F., 2002. Elevated mercury accumulation in a peat bog of the Magellanic Moorlands, Chile (53°S) - an anthropogenic signal from the Southern Hemisphere. Earth Planet. Sci. Lett. 201, 609–620.

Billups, K., 2015. Timing is everything during deglaciations. Nature 522, 163–164.

Carrie, J., Wang, F., Sanei, H., Macdonald, R.W., Outridge, P.M., Stern, G.A., 2010. Increasing contaminant burdens in and Arctic fish, Burbot (*Lota lota*), in a warming climate. Environ. Sci. Technol. 44, 316–322.

Cordeiro, R.C., Turcq, B., Riberio, M.G., Lacerda, L.D., Capitâneo, J., Silva, A.O., Sifeddine, A., Turcq, P.M., 2002. Forest fire indicators and mercury deposition in an intense land use change region in the Brazilian Amazon (Alta Floresta, MT). Sci. Total Environ. 293, 247–256.

Cordeiro, R.C., Turcq, B., Sifeddine, A., Lacerda, L.D., Silva Filho, E.V., Gueiros, B., Potty, Y.P., Santelli, R.E., Pádua, E.O., Pachinelam, S.R., 2011. Biogeochemical indicators of environmental changes from 50 ka to 10 ka in a humid region of the Brazilian Amazon. Palaeogeogr. Palaeoclimatol. Paleaeoecol. 299, 426–436.

Engstrom, D.R., Fitzgerald, W.F., Cooke, C.A., Lamborg, C.H., Drevnick, P.E., Swain, E.B., Balogh, S.J., Balcom, P.H., 2014. Atmospheric Hg emissions from preindustrial gold and silver extraction in the Americas: a reevaluation from lake-sediment archives. Environ. Sci. Technol. 48, 6533–6543.

Fritz, S.J., Toth, T.A., 1997. An Fe Bertierine from a cretaceous laterite. Part II: estimation of Eh, pH and $_pCO_2$ conditions of formation. Clays Clay Minerals 45, 580–586.

Grasby, S.E., Sanei, H., Beauchamp, B., Chen, Z.H., 2013. Mercury deposition through the permo-triassic biotic crisis. Chem. Geol. 351, 209–216.

Hacon, S., Artaxo, P., Gerab, F., Yamasoe, M.A., Campos, R.C., Conti, L.F., Lacerda, L.D., 1995. Atmospheric mercury and trace elements in the region of Alta Floresta in the Amazon basin. Water, Air & Soil Pollut. 80, 273–283.

Hermanns, Y.-M., Biester, H., 2013. A 17,300-year record of mercury accumulation in a pristine lake in southern Chile. J. Paleolimnol. 49, 547–561.

Jacob, J., Disnar, J.R., Boussafir, M., Sifeddine, A., Albuquerque, A.L.S., Turcq, B., 2004. Major environmental changes recorded by lacustrine sedimentary organic matter since the Last Glacial Maximum under the tropics (Lagoa do Caçó, NE Brazil). Palaeogeogr. Palaeoclimatol. Palaeoecol. 205, 183–197.

Jitaru, P., Gabrielli, P., Marteel, A., Plane, J.M.C., Planchon, F.A.M., Gauchard, P.A., Ferrari, C.P., Boutron, C.F., Adams, F.C., Hong, S., Cescon, P., Barbante, C., 2009. Atmospheric depletion of mercury over Antarctica during glacial periods. Nat. Geosci. 2, 505–508.

Lacerda, L.D., Salomons, W., 1998. Mercury from Gold and Silver Mining: a Chemical Time Bomb? Springer, Berlin, 146 p.

Lacerda, L.D., Ribeiro, M.G., 2004. Changes in lead and mercury loads to southeastern Brazil due to industrial emissions during the 20th century. J. Braz. Chem. Soc. 15, 931–937.

Lacerda, L.D., Ribeiro, M.G., Cordeiro, R.C., Sifeddine, A., Turcq, B., 1999. Mercury atmospheric deposition during the past 30,000 years in Brazil. J. Braz. Soc. Adv. Sci. 51, 363–371.

Lacerda, L.D., Bastos, W.R., 2012. The impacts of land use changes in the mercury flux in the Madeira River, Western Amazon. Anais da Academia Brasileira de Ciências 84, 69–78.

Lambert, F., Delmonte, B., Petit, J.R., Bigler, M., Kaufmann, P.R., Hutterli, M.A., Stocker, T.F., Ruth, U., Steffensen, J.P., Maggi, V., 2008. Dust-climate couplings over the past 800,000 years from the EPICA Dome C ice core. Nature 452, 616–619.

Ledru, M.-P., Cordeiro, R.C., Dominguez, J.M.L., Martin, L., Mourguiart, P., Sifeddine, A., Turcq, B., 2001. Late-glacial cooling in Amazonia inferred from pollen at Lagoa do Caçó, northern Brazil. Quat. Res. 55, 47–56.

Mayewski, P.A., Meeker, L.D., Twickler, M.S., Whitlow, S.I., Yang, Q., Lyons, W.B., Prentice, M., 1997. Major features and forcing of high-latitude features northern hemisphere atmospheric circulation using a 110,000-year-long glaciochemical series. J. Geophys. Res. 102, 26345–26366.

Nriagu, J.O., 1994. Mercury pollution from the past mining of gold and silver in the Americas. Sci. Total Environ. 149, 167–181.

Pérez-Rodríguez, M., Horak-Terra, I., Rodríguez-Lado, L., Aboal, J.R., Cortizas, A.M., 2015. Long-Term (~57 ka) controls on mercury accumulation in the southern hemisphere reconstructed using a peat record from Pinheiro Mire (Minas Gerais, Brazil). Environ. Sci. Technol. 49, 1356–1364.

Pyle, D.M., Mather, T.A., 2003. The importance of volcanic emissions for the global atmospheric mercury cycle. Atmos. Environ. 37, 5115–5124.

Roos-Barraclough, F., Martinez-Cortizas, A., García-Rodeja, E., Shotyk, W., 2002. A 14 500 year record of the accumulation of atmospheric mercury in peat: volcanic signals, anthropogenic influences and a correlation to bromine accumulation. Earth Planet. Sci. Lett. 202, 435–451.

Sanei, H., Grasby, S.E., Beauchamp, B., 2012. Latest Permian mercury anomalies. Geology 40, 63–66.

Santos, G.M., Cordeiro, R.C., Silva Filho, E.V., Turcq, B., Lacerda, L.D., Fifield, L.K., Gomes, P.R.S., Hausladen, P.A., Sifeddine, A., 2001. Chronology of atmospheric mercury in Lagoa da Pata Lake, upper Rio Negro region of Brazilian Amazon. Radiocarbon 43, 801–808.

Schuster, P.F., Krabbenhoft, D.P., Naftz, D.L., Cecil, L.D., Olson, M.L., Dewild, J.F., Susong, D.D., Green, J.R., Micheal, L.A., 2002. Atmospheric mercury deposition during the last 270 years: a glacial ice core record of natural and anthropogenic sources. Environ. Sci. Technol. 36, 2303–2310.

Sial, A.N., Lacerda, L.D., Ferreira, V.P., Frei, R., Marquillas, R.A., Barbosa, J.A., Gaucher, C., Windmöller, C.C., Pereira, N.S., 2013. Mercury as a proxy for volcanic activity during extreme environmental turnover: the Cretaceous-Paleogene transition. Palaeogeogr. Palaeoclimatol. Palaeoecol. 387, 153–164.

Sial, A.N., Chen, J., Lacerda, L.D., Peralta, S., Gaucher, C., Frei, R., Ferreira, V.P., Marquillas, R.A., Barbosa, J.A., Pereira, N.S., Belmino, I.K., 2014. High-resolution Hg Chemostratigraphy: a contribution to the distinction of chemical fingerprints of the Deccan volcanism and Cretaceous–Paleogene Boundary impact event. Palaeogeogr. Palaeoclimatol. Palaeoecol. 414, 98–115.

Sifeddine, A., Albuquerque, A.L.S., Ledru, M.-P., Turcq, B., Knoppers, B., Martin, L., Zamboni de Mello, W., Passenau, H., Cordeiro, R.C., Abrão, J.J., Bittencourt, A.C., 2003. A 21000 cal years paleoclimatic record from Caçó Lake, northern Brazil: evidence from sedimentary and pollen analyses. Palaeogeogr. Palaeoclimatol. Palaeoecol. 189, 25–34.

Sifeddine, A., Meyers, P.A., Cordeiro, R.C., Albuquerque, A.L., Bernardes, M., Turcq, B., Abrão, J.J., 2011. Delivery and deposition of organic matter in surface sediments of Lagoa do Caçó (Brazil). J. Paleolimnol. 45, 385–396.

Strode, S., Jaegle, L., Selin, N.E., 2009. Impact of mercury emissions from historic gold and silver mining: global modeling. Atmos. Environ. 43, 2012–2017.

Stuiver, M., Reimer, P.J., 1993. Extended ^{14}C data base and revised Calib 3.0 ^{14}C age calibration program. Radiocarbon 35, 215–230.

Sun, L., Yin, X., Liu, X., Zhu, R., Xie, Z., Wang, Y., 2006. 2000-year record of mercury and ancient civilizations in seal hairs from King George Island, West Antarctica. Sci. Total Environ. 368, 236–247.

Taylor, K.C., Mayewski, P.A., Twickler, M.S., Whitlow, S.I., 1996. Biomass and burning recorded in the GISP2 ice core: a record from eastern Canada? Holocene 6, 1–6.

UNEP, 2013. Global Mercury Assessment 2013: Sources, Emissions, Releases and Environmental Transport. UNEP Chemicals Branch, Geneva, Switzerland.

Vandal, G.M., Fitzgerald, W.F., Boutron, C.F., Candelone, J.P., 1993. Variations in mercury deposition to Antarctica over the past 34,000 years. Nature 362, 621–623.

Zielinski, G.A., Mershon, G.R., 1997. Paleoenvironmental implications of the insoluble microparticle record in the GISP2 (Greenland) ice core during the rapidly changing climate of the Pleistocene-Holocene transition. Geol. Soc. Am. Bull. 109, 547–559.

Zielinski, G.A., Mayewski, P.A., Meeker, L.D., Whitlow, S.I., Twickler, M.S., 1996. A 110,000-year record of explosive volcanism from the GISP2 (Greenland) ice core. Quat. Res. 45, 109–118.